University of New Hampshire
University of New Hampshire Scholars' Repository

Earth Sciences Scholarship

Earth Sciences

2-27-2003

Seasonal distributions of fine aerosol sulfate in the North American Arctic basin during TOPSE

Eric Scheuer
University of New Hampshire - Main Campus, Eric.Scheuer@unh.edu

R. Talbot
University of New Hampshire, robert.talbot@unh.edu

Jack E. Dibb
University of New Hampshire, jack.dibb@unh.edu

Garry Seid
University of New Hampshire - Main Campus

Linsey J. Debell
University of New Hampshire - Main Campus

See next page for additional authors

Follow this and additional works at: https://scholars.unh.edu/earthsci_facpub

Part of the Atmospheric Sciences Commons

Recommended Citation

Scheuer, E., R. W. Talbot, J. E. Dibb, G. K. Seid, L. DeBell, and B. Lefer (2003), Seasonal distributions of fine aerosol sulfate in the North American Arctic basin during TOPSE, J. Geophys. Res., 108, 8370, doi:10.1029/2001JD001364, D4.

Authors

Eric Scheuer, R. Talbot, Jack E. Dibb, Garry Seid, Linsey J. Debell, and Barry Lefer

Seasonal distributions of fine aerosol sulfate in the North American Arctic basin during TOPSE

Eric Scheuer, Robert W. Talbot, Jack E. Dibb, Garry K. Seid, and Linsey DeBell

Institute for the Study of Earth, Oceans and Space, University of New Hampshire, Durham, New Hampshire, USA

Barry Lefer

Atmospheric Chemistry Division, NCAR, Boulder, Colorado, USA

[1]   We used the mist chamber/ion chromatography technique to quantify fine aerosol $SO_4^=$ (<2.7 μm) in the Arctic during the Tropospheric Ozone Production about the Spring Equinox Experiment (TOPSE) with about 2.5 min time resolution. Our effective sample area ranged from 50° to 86°N and 53° to 100°W. The seasonal evolution of fine aerosol sulfate in the Arctic troposphere during TOPSE was consistent with the phenomenon of Arctic haze. Arctic haze has been attributed to pollution from sources in the Arctic and pollution transported meridionally along stable isentropes into the Arctic in geographically broad but vertically narrow bands. These layers became more prevalent at higher altitudes as the season progressed toward summer, and the relevant isentropes are not held so close to the surface. Mean fine particle $SO_4^=$ mixing ratios during TOPSE in February below 1000 m were elevated (112 pptv) and highly variable (between 28 and 290 pptv) but were significantly lower at higher altitudes (about 40 pptv). As the season progressed, elevated mixing ratios and higher variability were observed at higher altitudes, up to 7 km. In May, mixing ratios at the lowest altitudes declined but still remained higher than in February at all altitudes. The high variability in our measurements likely reflects the vertical heterogeneity of the wintertime Arctic atmosphere as the airborne sampling platform passed in and out of these layers. It is presumed that mixing ratios and variability will continue to decline at all altitudes into the summer as wet deposition processes become important in removing aerosol $SO_4^=$ from the troposphere.   *INDEX TERMS:* 0305 Atmospheric Composition and Structure: Aerosols and particles (0345, 4801); 0365 Atmospheric Composition and Structure: Troposphere—composition and chemistry; 0368 Atmospheric Composition and Structure: Troposphere—constituent transport and chemistry; 9315 Information Related to Geographic Region: Arctic region; *KEYWORDS:* TOPSE, fine sulfate, polar sunrise, mist chamber

1. Introduction

[2]   Accumulation of aerosols and anthropogenic pollutant gasses in the troposphere during the Arctic wintertime is well documented [*Rahn and Heidman*, 1981; *Barrie*, 1986]. The slow transformation and removal processes due to cold sub-zero temperatures, absence of wet precipitation, and low levels of solar radiation [*Barrie*, 1986] coupled with a slow, low- level, long-range meridional transport of Eurasian mid and high latitudinal pollutants into the Arctic lead to annual wintertime events which have become to be known as Arctic haze. This visual haze is largely due to the aerosol light scattering properties of accumulation mode particles [*Brock et al.*, 1989], which exhibit a dominant presence around the $0.01–0.5$ μm effective diameter range [*Blanchet and List*, 1983]. The hazes have been shown to be primarily of anthropogenic origin [*Radke and Hobbs*, 1984] with aerosol $SO_4^=$ constituting more than half of the total aerosol mass [*Shaw and Khalil*, 1989]. Most of this $SO_4^=$ mass is derived from anthropogenic emissions of SO_2 rather than primary particulate emissions [*Barrie and Hoff*, 1985]. Much of these emissions are believed to have originated from Europe and Russia [*Rahn and Heidman*, 1981] and been transported isentropically into the Arctic in multiday long pulses as low pressure systems run-up against the quasi-stationary Siberian high [*Barrie*, 1986].

[3]   Arctic Haze is believed to influence radiative budgets, snowpack albedo, snowpack chemical composition, and microphysical properties of Arctic clouds [*Brock et al.*, 1990]. Measurements of $SO_4^=$ aerosols in the Arctic have often been limited to geographically fixed locations. These data tend to be lacking information on spatial variability, both horizontally and vertically. Intensive airborne measurement campaigns conducted in both the summer (ABLE 3A-3B, 1988, 1990) and winter (AGASP I-IV, 1983, 1986, 1989, and
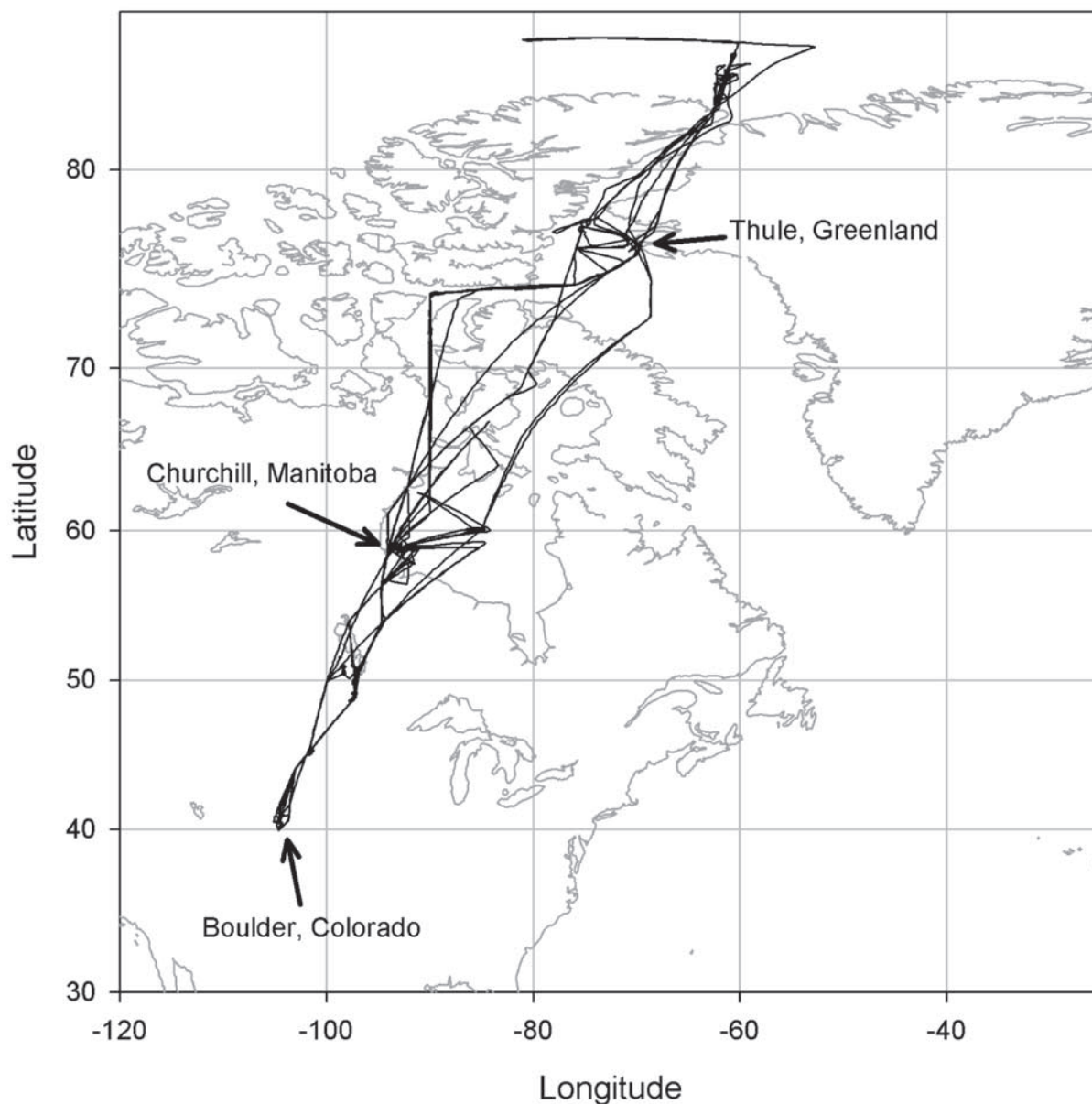
Figure 1. Flight track summary for all 42 flights conducted during TOPSE.

1991) into the Arctic have reported only a limited number of aerosol $SO_4^=$ measurements due to relatively long sample integration times inherent to filter collection techniques.

[4] In the early months of 2000, the heavily instrumented NSF/NCAR C-130 research aircraft conducted a series of trips into the Arctic beginning on February 4, 2000 and continuing until May 23, 2000. This campaign was called the Tropospheric Ozone Production about the Spring Equinox Experiment, or TOPSE. The primary objective of TOPSE was to study Arctic ozone production, loss and transport with a focus on the commonly observed springtime Arctic ozone maximum. It consisted of seven trips (42 total flights) from Boulder, Colorado (38°N) into the high Arctic environment (86°N). *Atlas et al.* [2003] provides an instrument payload description and detailed objectives of the flights conducted during TOPSE. A summary flight track plot including all flights conducted during TOPSE is shown as Figure 1.

[5] This field campaign provided an excellent opportunity to use the University of New Hampshire's dual mist chamber/ion chromatograph technique to examine the seasonal and vertical distributions of fine aerosol $SO_4^=$ in the Arctic. This technique was developed for the measurement of soluble gases such as HNO_3, CH_3COOH, $HCOOH$ [*Talbot et al.*, 1999], SO_2 [*Klemm and Talbot*, 1991], HCl [*Keene et al.*, 1993], and HONO [*Dibb*, 2003]. Experiments during prior intensive aircraft campaigns have demonstrated that with only minor modifications, measurements of fine soluble aerosols is possible. This technique is well suited for Arctic haze related aerosol $SO_4^=$ since the aerosols are present predominantly in the accumulation size mode [*Rahn and McCaffrey*, 1979; *Radke et al.*, 1984]. Previously, soluble aerosol sampling has been restricted to Teflon filter exposure and subsequent solvent/water extraction. The Teflon filter technique, although yielding more potential

analytes, suffers from long integration times, generally between 15 and 30 min. During the nearly 4-month period, 3820 samples were successfully collected using the mist chamber/ion chromatography technique with an average integrated collection time of 2.5 min. Analysis was performed in near-real time with detection limits as low as 4 parts per trillion by volume (pptv). To date, this was the most extensive $SO_4^=$ aerosol data set collected from an airborne platform.

[6] Twenty bulk aerosol measurements were made during TOPSE using the NCAR-RAF Small Community Aerosol Inlet (SCAI) and Teflon filters. These measurements were made primarily to help speciate detectable, but unexpected, amounts of soluble Br^- detected by the mist chamber/ion chromatograph system in many low altitude samples. Aerosol $SO_4^=$ was also detected and quantified in these samples, providing some measure of comparison to the mist chamber samples.

2. Methods

[7] A schematic representation of the University of New Hampshire mist chamber/ion chromatograph is presented as Figure 2. Soluble aerosols were collected in deionized water using two mist chambers operated alternately between a collection and analysis cycle similar to the system described by *Talbot et al.* [1999]. Operational descriptions of the mist chamber technique has been presented by *Cofer and Edahl* [1985], *Cofer et al.* [1986], *Talbot et al.* [1988], and *Talbot et al.* [1990]. Filters were not used on the sample inlet allowing aerosols to enter the sample stream. The mist chambers were connected to a sample manifold protruding from the aircraft about 25 cm, far enough to be in the free air stream and minimally affected by aircraft boundary layer effects. A 0.5-inch outer diameter inlet was positioned 90° to the airflow streamline over the aircraft, but was cut at a forward facing 45° angle. This 45° angle ensured that aerosol collected were small enough to make the 90° turn into the inlet, while larger particles were impacted on the inside face of the 45° cut. This design is believed to have excluded a majority of less radiatively important super-micron aerosols, commonly associated with sea salt and coarse mode dust. Based on particle stopping distance calculations taken from *Hinds* [1982] eqn.5.3 and 5.19, and an estimated average cruise speed of 129 m per second (250 KTAS), the median cutoff particle size sampled by our inlet is estimated to be about 2.7 μm. Although this is a slightly larger cutoff than was desired, it still excludes a large percentage of coarse mode particles. Indeed, the bulk of the mass distribution of $SO_4^=$ in the Arctic has been shown to be accumulation mode aerosol $SO_4^=$, centered on 0.3 μm [*Blanchet*, 1989]. We believe that we sampled this size range effectively. A more rigorous inlet design and validation routine, although desirable, was not attempted due to time, financial and airworthiness constraints coupled with the need to optimize passing of nitric acid (the species of primary interest to this instrument) in the same inlet.

[8] Chemical analysis of the samples collected by the mist chambers was conducted in near real-time using ion chromatography. The aqueous samples were removed from the mist chamber by computer controlled syringe pumps (Kloehn 50300) and injected into custom fabricated ion
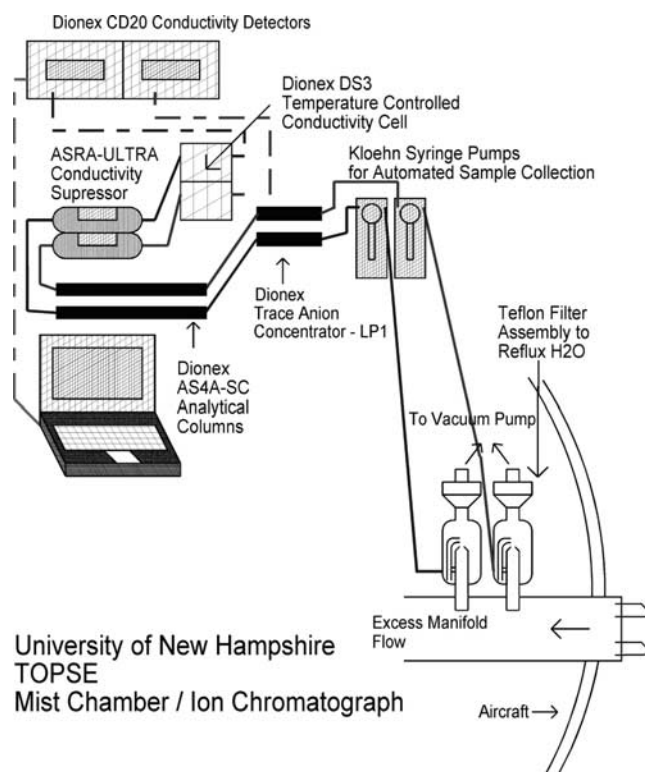

Figure 2. Schematic diagram of the two-channel mist chamber/ion chromatograph used during TOPSE.

chromatographs employing sample preconcentration (Dionex TAC-LP1). Separation was achieved using a helium purged carbonate/bicarbonate eluent and Dionex AS4A analytical columns. Background conductivity was suppressed using Dionex ASRS-Ultra suppressors. Detection of Cl^-, Br^-, NO_3^-, $SO_3^=$ and $SO_4^=$ was accomplished using a Dionex CD-20 conductivity detector equipped with a DS-3 temperature controlled cell. Sulfur dioxide is quickly converted in the mist chamber to aqueous sulfite ($SO_3^=$) which is easily detected by ion chromatography. Based on laboratory tests and sample stream filtering of $SO_4^=$, it has been determined that very little $SO_3^=$ is converted to $SO_4^=$ in the very short time between sample collection and analysis. Digitized data was then sent to a data acquisition computer using standard ethernet communications where post processing took place. An internal spike of known aqueous concentration of phosphate into the mist chamber and subsequent analysis was used to track any evaporative losses of water from the mist chamber during sampling. Two independent systems operated in tandem, which allowed for continuous sampling with an average 2.5-minute time resolution. It is important to note that, unlike conventional filter techniques, all sample and fluid handling was in a closed system and isolated from the aircraft cabin ambient air to prevent contamination.

3. Results

3.1. Filter Intercomparisons: Previous Missions

[9] During the 1999 NASA aircraft campaign Pacific Exploratory Mission - Tropics B (PEM-Tropics B) in the

South Pacific, we collected non-size selected aerosol $SO_4^=$ data using the standard Teflon filter technique and the mist chamber/ion-chromatography technique simultaneously. *Dibb et al.* [2003] describes the sampling methodology and presents some data for the samples collected using the Teflon filter technique. Filter exposure times averaged 14.2 min (σ = 7.2) on the DC-8 and 14.8 min (σ = 5.4) on the P3-B. Since the standard Teflon filter technique was designed for bulk aerosol sampling rather than a size selected fraction, some correction to make the data comparable was necessary. Although most non-marine aerosol $SO_4^=$ mass is in accumulation size mode [*Warneck*, 1988], there can be a significant fraction associated with sea-salt or crustal dust that is in the much larger coarse mode, especially in a marine environment. This makes a simple sea-salt correction to the total $SO_4^=$ an acceptable method to approximate the fine aerosol $SO_4^=$ (or non-sea salt) component. Magnesium was used as the sea-salt tracer element for the determination of sea-salt $SO_4^=$. *Keene et al.* [1986] presents a discussion of the use of sea-salt ratios for the determination of sea-salt and non sea-salt components of marine aerosols. Examples from the PEM-Tropics B experiment conducted in the South Pacific of the comparison between fine aerosol $SO_4^=$ (mist chamber/ion chromatograph) and non-sea salt $SO_4^=$ (Teflon filters) from both the NASA DC-8 and the NASA P3-B research aircraft are presented in Figure 3. A visual inspection of the data sets suggest that agreement between the two techniques is very good. The mist chamber/ion chromatography technique, however, exhibits much better time resolution than the Teflon Filter technique. This can be especially important during aircraft ascents and descents where a discrete sample represents a non-uniform altitude. Minimizing sample integration times becomes important in minimizing the vertical extent over which a sample is integrated. Filter samples are often not collected during ascents and descents because of this non-uniform altitude averaging issue.

3.2. Filter Intercomparisons During TOPSE

[10] The NCAR Small Community Aerosol Inlet (SCAI) with flow straightening shroud and a University of New Hampshire modified curved leading edge nozzle was employed during TOPSE to sample the aerosol associated radionuclide tracers ^{7}Be and ^{210}Pb [*Dibb*, 2003]. This inlet was also used to collect a limited number of bulk aerosol samples isokinetically on Teflon filters at low altitudes (<2 km asl). These samples were collected in order to facilitate speciation of soluble bromide observed in the mist chamber/ion chromatography analysis, however, aerosol $SO_4^=$ was also quantified in these samples. This provided a basis for comparison of TOPSE mist chamber/ion chromatography samples to bulk aerosol filer samples. Figure 4 shows excellent agreement in the $SO_4^=$ data when measured using the two techniques. The variability in the mist chamber data represents the standard deviation of the mean mixing ratio measured by the mist chamber during the approximately 15 minute time period that a bulk filter sample was being collected. It is not unexpected that the bulk aerosol data has a tendency to show slightly higher mixing ratios than the mist chamber data this close to the surface. Intercomparisons during the NASA PEM-Tropics B experiment suggest that agreement is even better at higher altitudes where $SO_4^=$

is almost exclusively on fine aerosols and uninfluenced by sea-salt or crustal dust.

3.3. Fine Aerosol $SO_4^=$ Measured During TOPSE

[11] A summary of the fine aerosol $SO_4^=$ data collected during TOPSE is presented in Table 1. The Table is restricted to latitudes greater than 50°N, since data collected south of 50°N were generally collected during transit flights to the primary study region. In order to examine the seasonal evolution of fine aerosol $SO_4^=$ in the Arctic, the data were summarized by trip and grouped into discrete 1000-m altitude bins in the latitude range of 50°N–86°N. Mixing ratios as high as 1766 pptv and as low as 4 pptv were observed during TOPSE (Table 1). The lowest values were generally observed during the first trip in early February. This trip also had the lowest variability in most altitude bins. The highest values were observed during the sixth trip in late April, which also exhibited the greatest variability.

[12] Our measured values are consistent with data presented by *Lazrus and Ferek* [1984] from the 1983 AGASP airborne sampling campaign. They report $SO_4^=$ concentrations in the Arctic as low as 7.3 neq/m^3 (82 pptv) and as high as 110 neq/m^3 (1233 pptv). Their samples, however, represent much longer periods of integration, and are less likely to represent a completely homogenous sample. That is, each one of their samples is more prone to have passed in and out of haze layers. This explains the smaller range of mixing ratios reported. Their highest value presented is reported to have been collected while flying in a continuous haze layer and may reflect a more homogeneous sample. Indeed, their highest mixing ratio reported is very similar to what we observed.

[13] The frequency distribution of our raw aerosol $SO_4^=$ data is highly skewed by less frequent but very high values. This can be explained by an abundance of cleaner air riddled with thin, highly polluted, layers. That is, since the polluted layers can be strongly delineated from the cleaner air, there appeared to be an absence of more moderate transition layers. Arithmetic means are only representative of data that has an approximately normal frequency distribution. This makes using arithmetic means for our $SO_4^=$ data bins very misleading. Using medians can have the opposite effect since the median is not very sensitive to our less frequently occurring, but very large observations. To address this problem, we use geometric means. This statistic can be applied since the data are more nearly lognormally distributed. This statistical tool addresses more of the real variability within the data set without placing emphasis on unusually high or low values. It also allows us to visualize real variability in the form of lognormally transformed standard deviations; presented graphically as unequal length error bars in Figure 5.

[14] During the first trip in early February, fine aerosol $SO_4^=$ mixing ratios were relatively low and not highly variable above 1000 m (Figure 5, top panel). Below 1000 m the range of mixing ratios was significantly higher and yielded a geometric mean of 110 pptv. This mean was more than two-fold higher than in any other altitude bin during this trip. Interestingly, *Ridley et al.* [2003] report a rarity of pollution events at very low altitude. $SO_4^=$ mixing ratios were, however, noticeably enhanced all the way to the
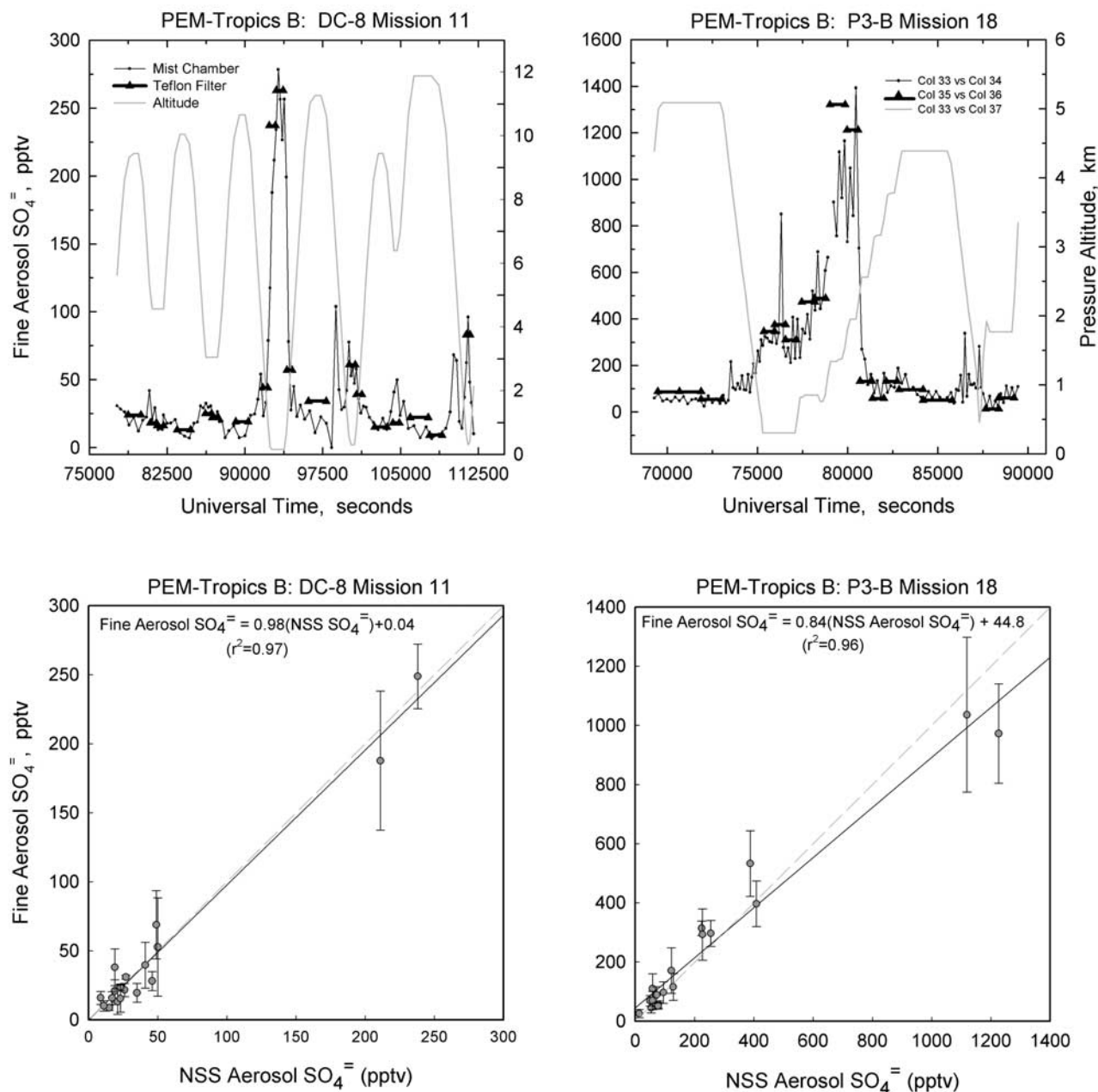
Figure 3. Example intercomparisons of non-sea-salt $SO_4^=$ mixing ratios from filter samples and fine aerosol $SO_4^=$ from the mist chamber technique on different aircraft during PEM-Tropics B. In the top panel time series plots, the length of the horizontal bars reflects filter exposure intervals. Mist chamber derived values are plotted at sample midpoint. The lower panels are scatterplots with least squaress regressions. For comparison, the dashed line is a 1:1 slope. Mixing ratios determined by the mist chamber technique (vertical axis) are averaged over the collection period of each filter (horizontal axis). Vertical error bars represent 1 standard deviation of mist chamber mixing ratios.

lowest altitudes surveyed during TOPSE throughout the campaign. *Barrie* [1986] reported data summarized by *Rahn and Heidman* [1981] noting that winter/spring pollution aerosols measured from a ground based Arctic aerosol sampling network averaged 2 μg/m3 $SO_4^=$ (466 pptv). This is consistent with our observations of near-surface $SO_4^=$ enhancements.

[15] During the second trip (late February), mean mixing ratios in the two lowest bins were almost double what was observed during the first trip, but mean mixing ratios above 2000 m remained around 50 pptv and were not highly variable. This trend of increasing mean mixing ratios at increasingly higher altitudes as the season progresses continued into trip 3 in early March. Mean mixing ratios below
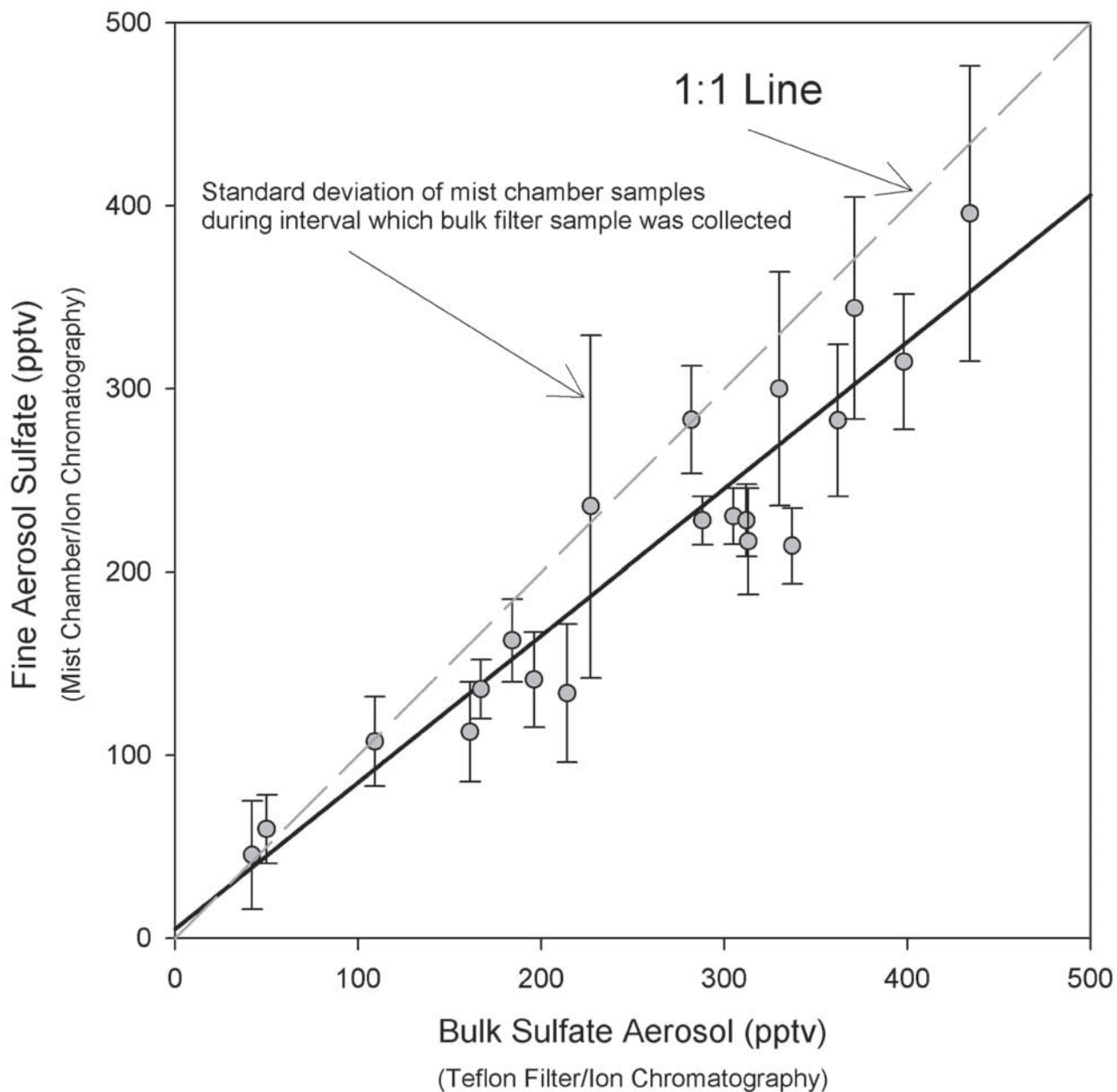
Figure 4. Intercomparison of the mist chamber/ion chromatograph technique to Teflon filter bulk aerosol $SO_4^=$ samples from TOPSE during periods of collection of the bulk aerosol samples. There were an average of 6 mist chamber samples collected for each of the approximately 15 minute bulk filter sample.

5000 m all appeared to be enhanced and increasingly variable with respect to earlier trips. There was also a gradient of about 70 pptv in mean mixing ratios (100 to 170 pptv) between the 2000 to 3000 m bin and below 1000 m.

[16] Mean mixing ratios were above 100 pptv in all altitude bins and above about 225 pptv below 2000 m by trip 4 in late March. The steepest gradient in $SO_4^=$ mean mixing ratio was no longer below 1000 m, but rather between 1000 and 3000 m. The trend of increasing mean mixing ratios in all altitude bins from trip to trip but decreasing mean mixing ratios with altitude began to show marked change during trip 5 in early April. Mean mixing ratios below 2000 m were lower than on the previous trip while mean mixing ratios above 2000 m continued to increase, albeit less dramatically. During the last two trips, fine aerosol sulfate mean mixing ratios generally continued to decrease below 3000 m and increase above 4000 m. By the end of the data collection phase of TOPSE, $SO_4^=$ mean mixing ratios showed no obvious altitude gradient and were greater thanthreefold higher at all altitudes above 1000 m than they were in early February (about 30 percent higher below 1000 m).

[17] *Talbot et al.* [1992] reported aerosol sulfate mixing ratios averaging 29 pptv in the boundary layer and 65 pptv

Table 1. Summary of Fine Aerosol Sulfate, North of 50-Degree Latitude, Binned by Trip and Altitude[a]

		Sample Count	Median (pptv)	Geometric Mean (pptv)	Minimum (pptv)	Maximum (pptv)
February 4–9 (Flights 5–8)						
Trip 1	<1000 m	31	124	112	28	290
	1000–2000 m	11	51	54	20	130
	2000–3000 m	21	58	61	18	188
	3000–4000 m	21	43	47	20	124
	4000–5000 m	17	43	41	16	131
	5000–6000 m	69	23	25	6	235
	6000–7000 m	10	23	19	12	25
	>7000 m	2	32	31	25	39
February 21–27 (Flights 9–13)						
Trip 2	<1000 m	59	165	155	48	406
	1000–2000 m	52	99	97	23	1766
	2000–3000 m	39	53	51	16	126
	3000–4000 m	29	59	49	12	132
	4000–5000 m	40	69	57	14	140
	5000–6000 m	113	50	50	18	150
	6000–7000 m	20	45	50	22	313
	>7000 m	28	39	44	21	103
March 5–8 (Flights 14–17)						
Trip 3	<1000 m	34	171	168	98	313
	1000–2000 m	14	117	142	44	552
	2000–3000 m	24	133	105	4	530
	3000–4000 m	13	117	83	8	543
	4000–5000 m	21	86	101	23	337
	5000–6000 m	35	50	46	8	189
	6000–7000 m	37	27	30	9	214
	>7000 m	15	43	37	12	117
March 19–26 (Flights 18–23)						
Trip 4	<1000 m	85	206	225	116	667
	1000–2000 m	58	242	219	19	540
	2000–3000 m	69	211	158	40	597
	3000–4000 m	40	133	129	34	446
	4000–5000 m	76	130	125	33	498
	5000–6000 m	110	126	109	47	473
	6000–7000 m	40	104	109	46	242
	>7000 m	51	116	118	49	268
April 2–7 (Flights 24–30)						
Trip 5	<1000 m	85	219	209	95	598
	1000–2000 m	43	212	217	76	504
	2000–3000 m	33	243	221	85	400
	3000–4000 m	33	200	194	87	364
	4000–5000 m	93	183	176	73	407
	5000–6000 m	110	129	122	43	324
	6000–7000 m	79	122	120	63	307
	>7000 m	26	131	136	59	313
April 23–30 (Flights 31–36)						
Trip 6	<1000 m	97	223	184	26	628
	1000–2000 m	48	189	208	78	597
	2000–3000 m	68	236	237	84	784
	3000–4000 m	40	191	171	33	842
	4000–5000 m	65	199	173	4	684
	5000–6000 m	168	157	140	57	1160
	6000–7000 m	25	172	199	69	698
	>7000 m	59	110	120	21	470
May 15–23 (Flights 37–42)						
Trip 7	<1000 m	70	173	149	21	322
	1000–2000 m	64	170	162	20	722
	2000–3000 m	45	187	143	10	788
	3000–4000 m	62	170	153	27	374
	4000–5000 m	61	175	157	36	417
	5000–6000 m	179	171	160	32	487
	6000–7000 m	58	128	124	30	390
	>7000 m	24	162	143	59	400

in the free troposphere during the ABLE 3A (1988) summer campaign in the Arctic. This suggests that $SO_4^=$ mixing ratios in the high Arctic should continue declining through late spring into the summer, possibly exhibiting a gradient inverse to that noted in the earlier TOPSE trips. This decrease must happen rapidly during the month of June, and is likely related to the onset of warmer temperatures and liquid precipitation.

[18] The seasonal evolution of aerosol $SO_4^=$ in the Arctic is shown in a different format in Figure 6. Mean mixing ratios of $SO_4^=$ below 2000 m increased during early February until the end of March, reaching a mean mixing ratio maximum of about 220 pptv. Mean mixing ratios declined to about 150 pptv during April and May. In the middle troposphere (2000–5000 m), mixing ratios continued to increase until the end of March, reaching a mean mixing ratio peak of 200 pptv. In the upper Arctic troposphere, mean mixing ratios appeared to still be increasing at the conclusion of the sampling campaign, but had not exceeded levels in the lower and middle troposphere (which were already declining from peak values). The sharp decreasing trends in mean mixing ratios in the lower and middle troposphere coupled with the still increasing or flat gradients in the upper troposphere would produce the summertime inverse gradient observed by *Talbot et al.* [1992].

[19] To examine latitudinal trends in aerosol $SO_4^=$ data collected during TOPSE, we binned data into two seasons (winter and spring) and three altitude bins (below 2000 m, 2000–5000 m, and above 5000 m). All values measured north of 50°N were plotted along with binned 5° latitude geometric means (Figure 7) to demonstrate the variability that characterized the Arctic troposphere. This extreme variability results from samples that were collected both in and out of haze layers. Mean mixing ratios appear to increase with latitude at all altitudes in both winter and spring, but only minimally. There is a more notably sharp gradient in minimum values measured north of about 70°N. This is especially evident in the lower troposphere in both the spring and winter. This trend in elevated minimum mixing ratios is also seen at higher altitudes, but the gradient is less steep. It does, however, continue to lower latitudes. This is consistent with, and a nice illustration of, the 7–8 km deep "polar dome" described by *Barrie* [1986] and *Shaw and Khalil* [1989].

4. Discussion

[20] The seasonal trend in vertical aerosol $SO_4^=$ distribution during TOPSE is clear in Figure 5. During early February, significant enhancements in aerosol $SO_4^=$ appear to be strongly confined near the surface. Long-range transport from the northern Eurasian continent along low level, sinking isentropes is likely most responsible for this observation. As the season progresses from winter to spring, this phenomenon of long-range isentropic transport begins to ascend vertically. Evidence that the polluted parcels of air

---

Notes to Table 1
[a]The geometric mean (M) commonly used for lognormally distributed data. It is the nth root of the product of the values in a given bin. $[M_{(x)} = (x_1 x_2 \ldots x_n)^{1/n}]$.
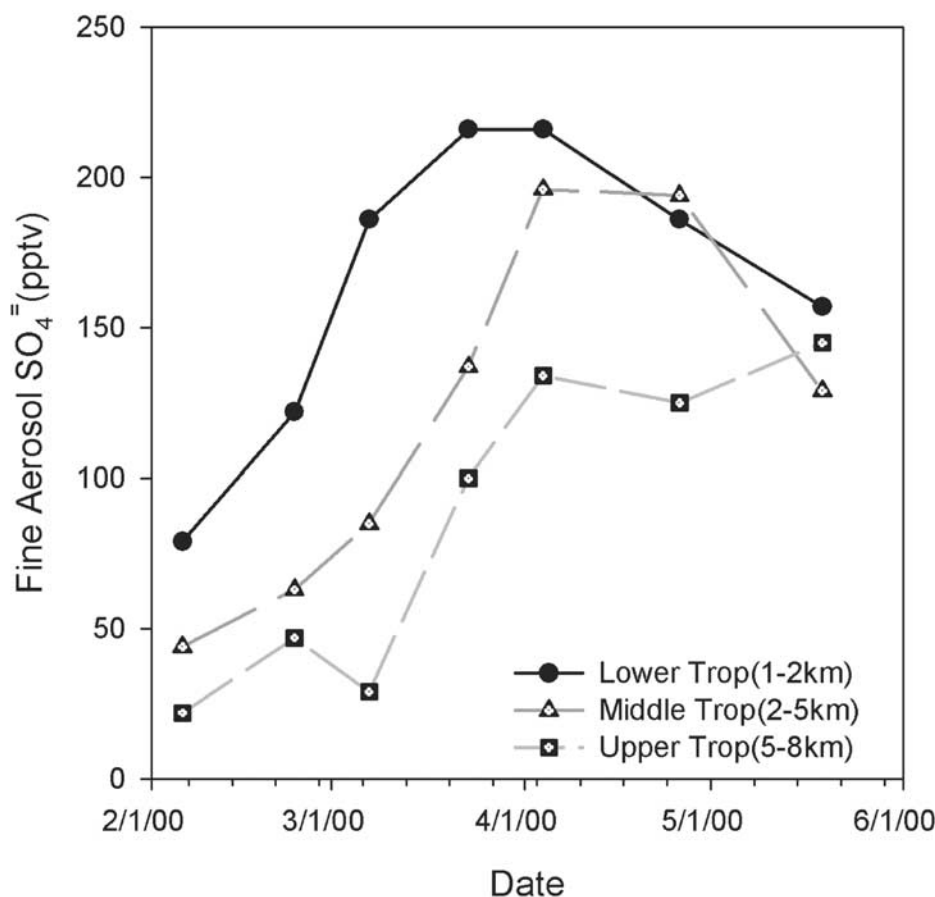
Fine Aerosol SO₄⁼ (pptv)
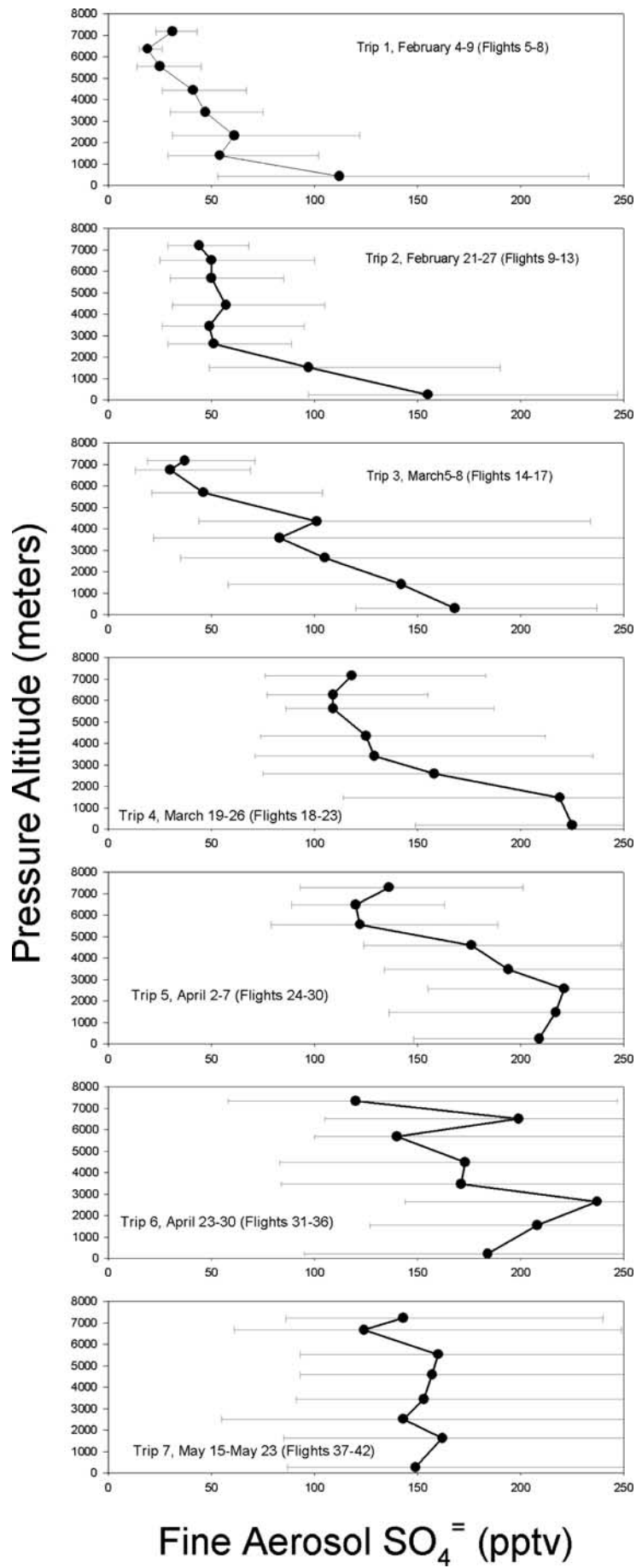
Figure 6. Seasonal progression of geometric mean mixing ratios of fine aerosol $SO_4^=$ in three altitude bins.

are confined to near the surface disappears as dramatically enhanced mixing ratios are observed at higher altitudes. We believe that, even in the late winter, vertical mixing is a small or non-existent component of the observed enhancement at higher elevations. Mixing of low-level air with the overlying free troposphere is inhibited by a persistent low-level inversion [*Kahl*, 1990]. Stable inversions can last for several weeks essentially decoupling the lower troposphere from higher altitudes [*Bradley et al.*, 1992]. Elevated mixing ratios at higher and higher altitudes as the season progresses must be explained by transport into the Arctic along vertically higher isentropes tracing back to warmer and warmer source regions in northern Eurasia. A discussion of isentropic transport pathways coupled with source region potential temperatures during TOPSE is presented by *Klonecki et al.* [2003].

[21] During early April, below 3000 m, levels of $SO_4^=$ enhancement began to decline. An increase in inversion base depths and decrease in inversion persistence probabilities [*Kahl et al.*, 1992] hint that solar surface heating may be beginning to stir up the lowest levels of the atmosphere while more stable isentropic transport can continue at higher

altitudes. Removal processes, dominated by wet deposition [*Barrie*, 1985], become increasingly important and decrease mixing ratios at lower altitudes. By the end of May, surface mixing ratios of fine aerosol $SO_4^=$ are almost half of the maximum observed in March. Mixing ratios also appear to be beginning to decrease at higher altitudes. This is consistent with the much lower values observed at all altitudes during summer months by *Talbot et al.* [1992].

[22] The high variability observed in Figure 5 demonstrate that $SO_4^=$ aerosol mixing ratios in the Arctic winter are far from homogeneous. Mixing ratios during the late February trip (trip 2) in the 1000–2000 m altitude bin were observed to be as low as 23 pptv and as high as 1766. This is consistent with prior observations of multiple narrow haze bands covering between 20–200 km [*Radke et al.*, 1984] which are often between tens of meters to 1 km thick, [*Brock et al.*, 1989] and streaming slowly into the Arctic environment. Individual altitude bins of data presented here probably incorporate both cleaner and more polluted layers, leading to high variability within the bins. The observations of increasing $SO_4^=$ mean mixing ratios in an altitude bin during the winter can be attributed to more frequent

---

Figure 5. (opposite) Vertical distributions of geometric mean mixing ratios between 50 and 85 north latitude. Error bars represent 1 standard deviation about the geometric mean and are therefore asymmetric. They represent a measure of variability of mixing ratios observed (about 68%) and not error.
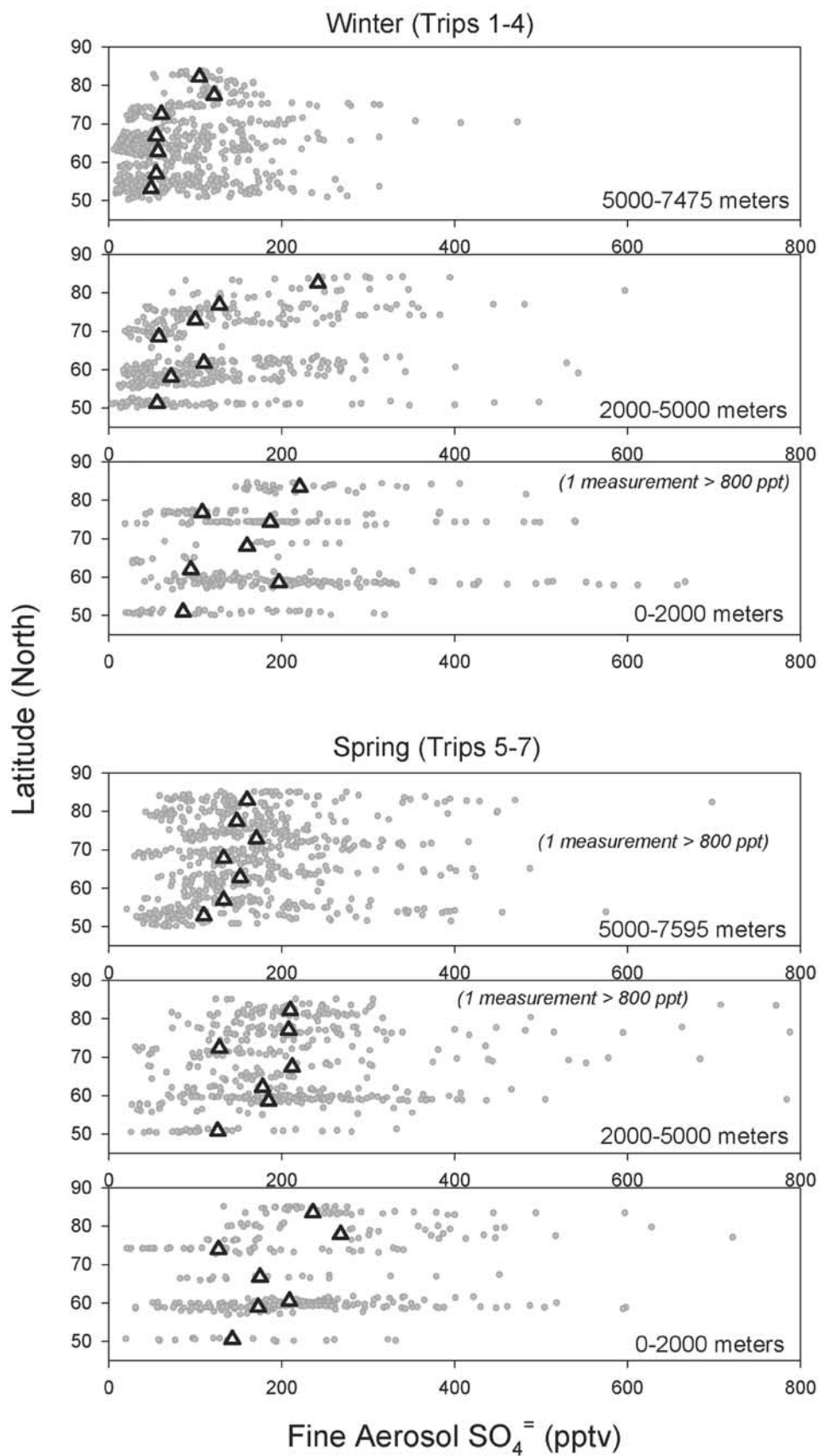
Figure 7. Latitudinal distributions of fine aerosol SO$_4^=$ during winter and spring in 3 altitude bins. Raw data shown (circles) are discrete measurements made north of 50°N. Triangles represent geometric means of SO$_4^=$ mixing ratios plotted at the mean latitude of the 5° bins.

occurrences of these narrow polluted layers within the bin region.

5. Conclusion

[23]   The mist chamber/ion chromatograph is shown to be an effective tool for the measurement of fine aerosol $SO_4^=$ aboard an aircraft platform. During TOPSE, we collected an extensive fine aerosol $SO_4^=$ data set. These measurements paint a four monthlong picture of the vertical distributions in the Arctic. Small-scale variability and poorly understood frequencies of haze layers, however, makes estimation of total aerosol burdens difficult [*Brock et al.*, 1990]. The slow transport, and lack of major chemical transformations, however, does allow us to treat the approximately weeklong measurement campaigns as synoptic snapshots of the Arctic environment. It is shown that $SO_4^=$ aerosols begin to build up at very low altitudes during the winter. The altitude at which the buildup is most pronounced tended to migrate to higher altitudes as the season progressed toward spring. In spring, $SO_4^=$ aerosols began to clean up at lower altitudes first, progressing upward. It is possible that much of the fine detail of the Arctic air is lost in the averaging and temporal gaps in the data. Follow-up investigations into the frequency, distribution, and spatial variability of Arctic pollution layers could help provide better information into the extent and magnitude of these layer as well as help better explain the extreme heterogeneity observed.

References

Atlas, E., B. Ridley, and C. Cantrell, The Tropospheric Ozone Production about the Spring Equinox experiment: Introduction, *J. Geophys. Res.*, 108, doi:10.1029/2002JD003172, in press, 2003.

Barrie, L. A., Atmospheric particles: Their physical and chemical characteristics, and deposition processes relevant to the chemical composition of glaciers, *Ann. Glaciol.*, 7, 100–108, 1985.

Barrie, L. A., Arctic air pollution: An overview of current knowledge, *Atmos. Environ.*, 20, 643–663, 1986.

Barrie, L. A., and R. M. Hoff, Five years of air chemistry observation in the Canadian Arctic, *Atmos. Environ.*, 19, 1995–2010, 1985.

Blanchet, J., Toward estimation of climatic effects due to arctic aerosols, *Atmos. Environ.*, 23, 2609–2625, 1989.

Blanchet, J., and R. List, Estimation of optical properties of arctic haze using a numerical model, *Atmos. Ocean*, 21, 444–465, 1983.

Bradley, R. S., F. T. Keimig, and H. F. Diaz, Climatology of surface-based inversions in the North American Arctic, *J. Geophys. Res.*, 97, 15,699–15,712, 1992.

Brock, C. A., L. F. Radke, J. H. Lyons, and P. V. Hobbs, Arctic hazes in summer over Greenland and the North American Arctic, I, Incidence and origins, *J. Atmos. Chem.*, 9, 129–148, 1989.

Brock, C. A., L. F. Radke, and P. V. Hobbs, Sulfur in particles in arctic hazes derived from airborne in situ and lidar measurements, *J. Geophys. Res.*, 95, 22,369–22,387, 1990.

Cofer, W. R., and R. A. Edahl, A new technique for collection, concentration and determination of gaseous tropospheric formaldehyde, *Atmos. Environ.*, 20, 979–984, 1985.

Cofer, W. R., V. G. Collins, and R. W. Talbot, Improved aqueous scrubber for collection of soluble atmospheric trace gases, *Environ. Sci. Technol.*, 19, 557–560, 1986.

Dibb, J. E., R. W. Talbot, G. Seid, C. Jordan, E. Scheuer, E. Atlas, N. J. Blake, and D. R. Blake, Airborne sampling of aerosol particles: Comparison between surface sampling at Christmas Island and P-3 sampling during PEM Tropics B, *J. Geophys. Res.*, 108(D2), 8230, doi:10.1029/2001JD000408, 2002.

Dibb, J. E., R. W. Talbot, E. Scheuer, G. Seid, and L. DeBell, Stratospheric influence on the northern North American free troposphere during TOPSE: ^{7}Be as a Stratospheric Tracer, *J. Geophys. Res.*, 108(D4), 8363, doi:10.1029/2001JD001347, 2003.

Hinds, W. C., Acceleration and curvilinear particle motion, in *Aerosol Technology*, pp. 105–110, John Wiley, New York, 1982.

Kahl, J. D., Characteristics of the low-level temperature inversion along the Alaskan Arctic coast, *Int. J. Climatol.*, 10, 537–548, 1990.

Kahl, J. D., M. C. Serreze, and R. C. Schnell, Tropospheric low-level temperature inversions in the Canadian Arctic, *Atmos. Ocean*, 30, 511–529, 1992.

Keene, W. C., A. P. P. Pszenny, J. N. Galloway, and M. E. Hawley, Sea-salt corrections and and interpretations of constituent ratios in marine precipitation, *J. Geophys. Res.*, 91, 6647–6658, 1986.

Keene, W. C., J. R. Maben, A. P. P. Pszenny, and J. N. Galloway, Measurement technique for inorganic chlorine gases in the marine boundary layer, *Environ. Sci. Tech.*, 27, 1993.

Klemm, O., and R. W. Talbot, A sensitive method for measuring atmospheric concentrations of sulfur dioxide, *J. Atmos. Chem.*, 13, 325–342, 1991.

Klonecki, A., P. Hess, and D. Blake, Seasonal changes in the transport of pollutants into the Arctic troposphere- model study, *J. Geophys. Res.*, 108, doi:10.1029/2002JD002199, in press, 2003.

Lazrus, A. L., and R. J. Ferek, Acidic sulfate particles in the winter arctic atmosphere, *Geophys. Res. Lett.*, 11, 417–419, 1984.

Radke, F. L., and P. V. Hobbs, Airborne observations of arctic aerosols, III, Origins and effects of airmasses, *Geophys. Res. Lett.*, 11, 401–404, 1984.

Radke, F. L., J. H. Lyons, D. A. Hegg, P. V. Hobbs, and I. H. Bailey, Airborne observations of arctic aerosols, I, Characteristics of arctic haze, *Geophys. Res. Lett.*, 11, 393–396, 1984.

Rahn, K. A., Relative importances of North America and Eurasia as sources of Arctic aerosol, *Atmos. Environ.*, 15, 1447–1455, 1981.

Rahn, K. A., and R. J. McCaffrey, Long-range transport of pollution aerosol to the Arctic: A problem without boarders, paper presented at the WMO Symposium on the Long Range Transport of Pollutants and its Relation the General Circulation Including Stratospheric/Tropospheric Exchange Processes, World Meteorol. Org., Sofia, Bulgaria, 1–5 October 1979, 1979.

Rahn, K. A., and N. Z. Heidman, Progress in Arctic air chemistry, 1977–1980: A comparison of the first and second symposia, *Atmos. Environ.*, 15, 1345–1348, 1981.

Ridley, B. A., et al., Ozone depletion events observed in the high latitude surface layer during the TOPSE aircraft program, *J. Geophys. Res.*, 108(D4), 8356, doi:10.1029/2001JD001507, 2003.

Shaw, G. E., and M. A. K. Khalil, Arctic haze, *The Handbook of Environmental Chemistry*, vol. 4, edited by O. Hutzinger, pp. 89–91, Springer-Verlag, New York, 1989.

Talbot, R. W., K. M. Beecher, R. C. Harriss, and W. R. Cofer, Atmospheric geochemistry of formic and acetic acids at a mid-latitude temperate site, *J. Geophys. Res.*, 93, 1638–1652, 1988.

Talbot, R. W., A. S. Vijgen, and R. C. Harriss, Measuring tropospheric HNO_3: Problems and prospects for nylon filter and mist chamber techniques, *J. Geophys. Res.*, 95, 7553–7561, 1990.

Talbot, R. W., A. S. Vijgen, and R. C. Harriss, Soluble Species in the arctic summer troposphere: Acidic gases, aerosols, and precipitation, *J. Geophys. Res.*, 97, 16,531–16,543, 1992.

Talbot, R. W., et al., Reactive nitrogen budget during the SONEX mission, *Geophys. Res. Lett.*, 20, 3057–3060, 1999.

Warneck, P., Sulfur compounds in the atmosphere, in *Chemistry of the Natural Atmosphere*, vol. 41, pp. 484–542, Academic, San Diego, Calif., 1988.

———————————

L. DeBell, J. E. Dibb, E. Scheuer, G. K. Seid, and R. W. Talbot, Institute for the Study of Earth, Oceans and Space, University of New Hampshire, Durham, NH, USA. (eric.scheuer@unh.edu)

B. Lefer, Atmospheric Chemistry Division, National Center for Atmospheric Research, P. O. Box 3000, 1850 Table Mesa Drive, Boulder, CO 80305, USA.